ELSEVIER

Chemical Geology 237 (2007) 28–46

CHEMICAL GEOLOGY
INCLUDING
ISOTOPE GEOSCIENCE

www.elsevier.com/locate/chemgeo

Chemostratigraphy of the Cerro Victoria Formation (Lower Cambrian, Uruguay): Evidence for progressive climate stabilization across the Precambrian–Cambrian boundary

Claudio Gaucher [a,*], Alcides N. Sial [b], Valderez P. Ferreira [b], Marcio M. Pimentel [c], Leticia Chiglino [a], Peter Sprechmann [a]

[a] *Departamento de Geología, Facultad de Ciencias, Iguá 4225, 11400 Montevideo, Uruguay*
[b] *NEG-LABISE, Departamento de Geología, Universidade Federal de Pernambuco (UFPE), C.P. 7852, Recife-PE, 50670–000, Brazil*
[c] *Instituto de Geociencias, Universidade de Brasilia, Brasília-DF, 70910–900, Brazil*

Accepted 8 June 2006

Editor: P. Deines

Abstract

Petrographic, isotopic and geochemical data are reported for the Cerro Victoria Formation of the Arroyo del Soldado Group (Uruguay). It is divided into four informal lithostratigraphic units (A to D), which are mainly composed of an alternation of stromatolitic, oolitic and clastic dolostones. The genesis of dolomite as a primary or penecontemporaneous precipitate is discussed, considering excellent preservation of textural details. Whereas $^{87}Sr/^{86}Sr$ ratios in the least altered samples are too high (0.7106–0.7109) to represent seawater values, $\delta^{13}C$ determinations are interpreted as reflecting near-seawater composition. The curve obtained for the Cerro Victoria Formation is characterized by negative values at its base (−3.5‰$_{PDB}$), passing into a slightly positive plateau up section. Peak values of +0.64‰$_{PDB}$ are encountered in the upper unit C. The upper Cerro Victoria Formation is characterized by a return to moderately negative values. The shape of the $\delta^{13}C$ curve is consistent with the data reported for the Nemakit–Daldyn stage of the Lower Cambrian. We suggest that the Precambrian/Cambrian boundary is located at the Cerros San Francisco–Cerro Victoria transition or slightly lower in the succession. *Thalassinoides*-bearing dolostones of the upper Cerro Victoria Formation might reach the Tommotian or Atdabanian. In the Arroyo del Soldado Group, $\delta^{13}C$ excursions parallel sea-level oscillations, transgressive events being characterized by positive $\delta^{13}C$ values. Falling amplitudes of coupled $\delta^{13}C$/sea-level fluctuations recorded in these carbonates are in accordance with the trend observed in Ediacaran–Lower Cambrian successions worldwide. Covariance of $\delta^{13}C$ and sea-level might be explained by bioproductivity fluctuations affecting the carbon cycle, atmospheric CO_2 concentrations, climate, ice-volume and ultimately sea-level. While these oscillations were of large magnitude in the late Neoproterozoic, they progressively faded away in the Cambrian, giving place to a more stable environment. The cause of the amplitude decrease in biogeochemical, climatic and sea-level perturbations might be the decreasing rates of nutrient input at mid-ocean ridges, as reflected by rising $^{87}Sr/^{86}Sr$ values between 800 and 500 Ma, punctuated by at least three events roughly coincident with rifting episodes of Rodinia.

Keywords: Cambrian; Neoproterozoic; Uruguay; Chemostratigraphy; Dolomite

* Corresponding author. Fax: +598 2 5258617.
E-mail address: gaucher@chasque.net (C. Gaucher).

0009-2541/$ - see front matter © 2006 Elsevier B.V. All rights reserved.
doi:10.1016/j.chemgeo.2006.06.014

1. Introduction

The Arroyo del Soldado Group (ASG) is a 5 km-thick platform succession unconformably overlying Archean to Mesoproterozoic basement (Nico Pérez Terrane, Fig. 1) in central-eastern Uruguay (Gaucher et al., 1996, 1998; Gaucher, 2000; Figs. 1 and 2). The group is characterized by an alternation of predominantly siliciclastic (Yerbal, Cerro Espuelitas, Barriga Negra and Cerros San Francisco Formations) and carbonate units (Polanco and Cerro Victoria Formations, Fig. 3). Carbonates were deposited on pericontinental, storm-dominated carbonate ramps. Siliciclastic units were deposited in a basin with gentle palaeoslope; sandstones are texturally and mineralogically mature quartzarenites or subarkoses (Gaucher, 2000). Altogether, these facts strongly suggest a stable, Atlantic-type continental margin as the geotectonic setting of the Arroyo del Soldado basin (Gaucher, 2000).

The ASG is notable for its extensive and very thick carbonate deposits, namely (a) the Polanco Formation, more than 900 m in maximum thickness (Gaucher et al., 2004a), (b) the Cerro Victoria Formation, composed of up to 400 m of stromatolitic, oolitic and micritic dolostones, and (c) various isolated dolostone and limestone strata in the lower Cerro Espuelitas and upper Yerbal formations (Fig. 3). These provide excellent proxies for chemostratigraphic studies in a time of extreme biogeochemical oscillations, environmental instability and biological innovations. Carbon and oxygen isotopic data from the ASG have been previously reported by Boggiani (1998), Kawashita et al. (1999), Gaucher (2000) and Gaucher et al. (2003, 2004a). Kawashita el al. (1999) presented four Sr-isotopic determinations for the lower Polanco Formation. We report here the results of a series of thirty-one C- and O-isotopic determinations and fourteen $^{87}Sr/^{86}Sr$ analyses on carbonates of the Cerro Victoria Formation as well as geochemical and petrographic data, and discuss their palaeoenvironmental and chemostratigraphic implications.

2. Age constraints

The age of the ASG is geochronologically constrained by: (a) a maximum U–Pb SHRIMP age of 633±12 Ma for the Puntas del Santa Lucía pluton (Hartmann et al., 2002), which is overlain with erosional unconformity by

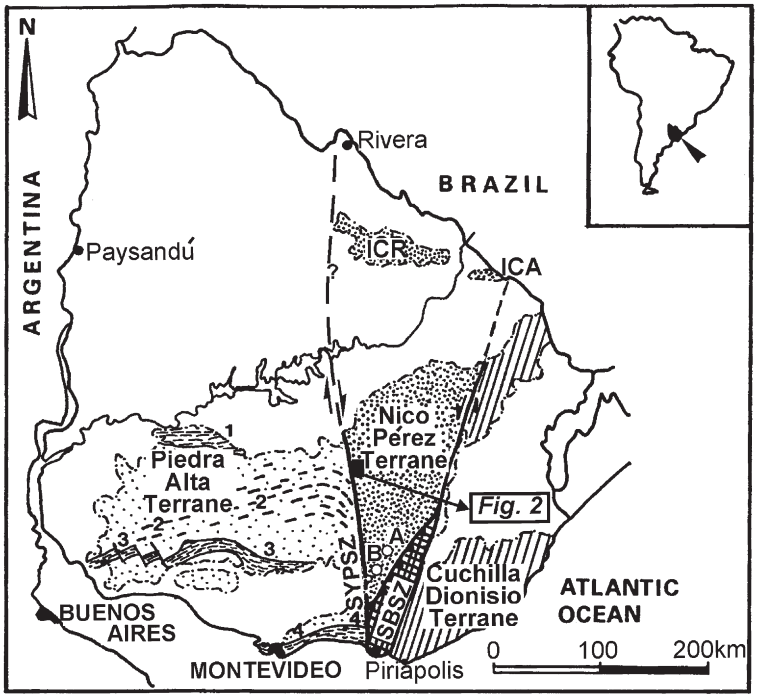

Fig. 1. Tectonostratigraphic subdivision of the Precambrian of Uruguay according to Bossi and Campal (1992), Gaucher et al. (1998) and Bossi et al. (1998). SYPSZ: Sarandí del Yí-Piriápolis Shear Zone; SBSZ: Sierra Ballena Shear Zone; ICR: Isla Cristalina de Rivera; ICA: Isla Cristalina de Aceguá. 1, 3 and 4: Palaeoproterozoic metamorphic belts. 2: Río de la Plata mafic dyke swarm. Note location of work area shown in Fig. 2. Points A and B indicate location of sections shown in Fig. 4. Modified from Gaucher (2000).

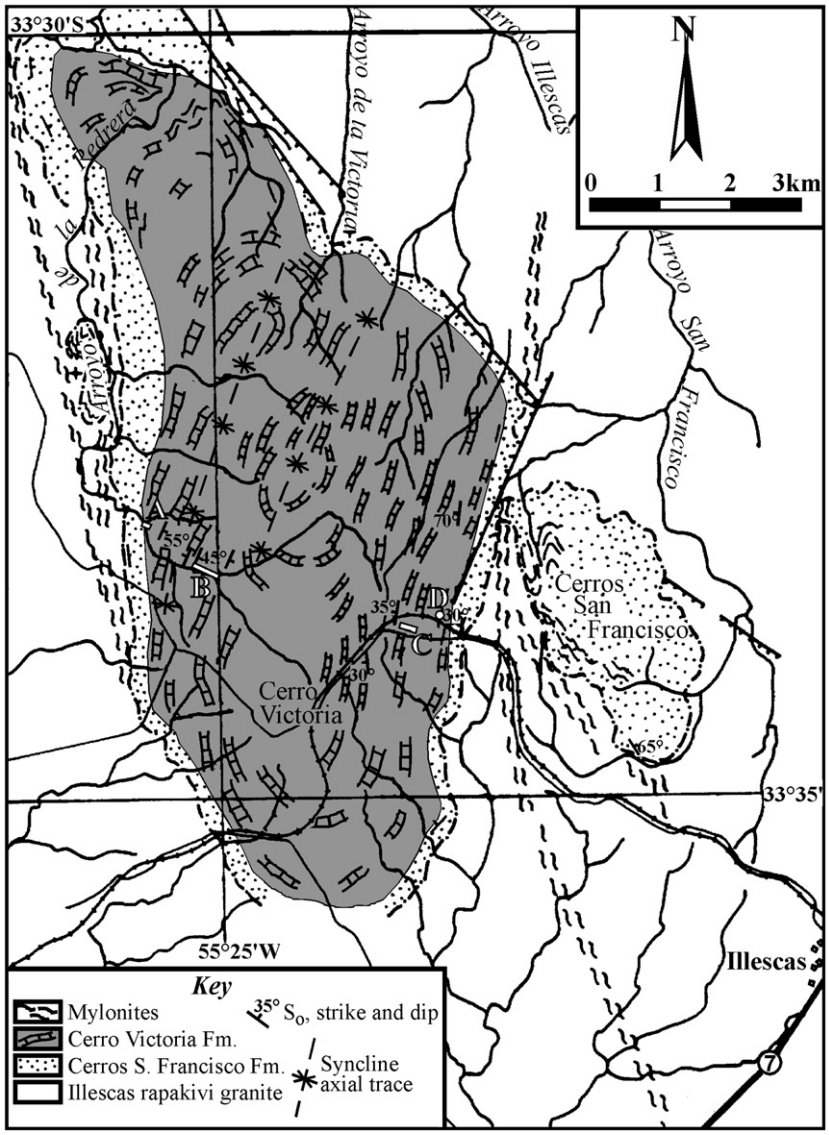

Fig. 2. Geological map of the Arroyo de la Pedrera Syncline. A, B and C: sections measured and sampled in this study (Figs. 5, 9). D: outcrop showing the Cerros San Francisco–Cerro Victoria transition. Mylonites shown belong to the Sarandí del Yí-Piriápolis shear system (Fig. 1).

the ASG; and (b) a minimum Rb–Sr isochron age for the Guazunambí Granite of 532±11 Ma (R_o=0.70624: Kawashita et al., 1999), which intrudes into the ASG causing contact-metamorphism. Additional data are provided by K–Ar ages ranging between 532±16 and 492±14 Ma for the recrystallization of pelites belonging to the group (Cingolani et al., 1990; Gaucher, 2000).

Biostratigraphic data also point to an upper Ediacaran (Vendian) age for the lower–middle ASG, and a lowermost Cambrian age for the Cerro Victoria Formation (Fig. 3). An assemblage of skeletal fossils containing *Cloudina riemkeae* Germs (1972), *Titanotheca coimbrae* Gaucher and Sprechmann (1999) and at least five other genera- and species occurs in the uppermost Yerbal Formation of the ASG (Gaucher and Sprechmann, 1999; Gaucher, 2000; Fig. 3). *Cloudina* is recognized as an index-fossil of the upper Vendian (Grant, 1990), and has a global distribution in rocks of that age (Gaucher et al., 2003 and references therein). A low-diversity, high-abundance assemblage of organic-walled microfossils is preserved in the ASG as well (Gaucher et al., 1996, 1998; Gaucher, 2000). *Bavlinella faveolata*, *Soldadophycus bossii* and *S. major* are dominant in the siliciclastic units, while in the Polanco Formation a slightly more diverse assemblage (*Leiosphaeridia–Lophosphaeridium* assemblage) occurs

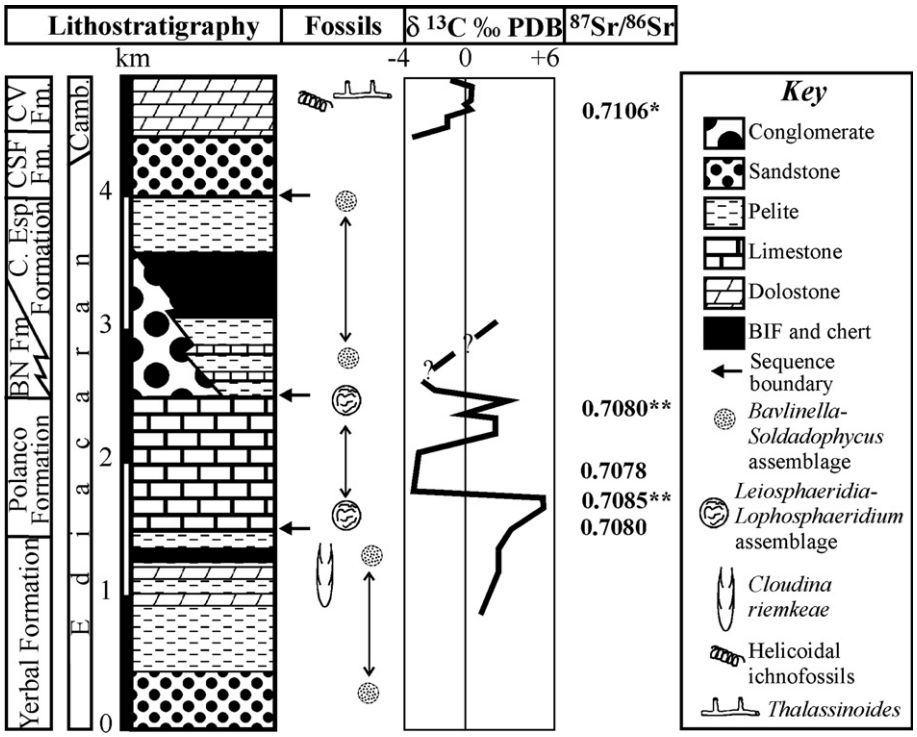

Fig. 3. Litho-, bio- and chemostratigraphy of the Arroyo del Soldado Group, according to Gaucher (2000) and Gaucher et al. (2003, 2004a). Sr-isotopic data after Kawashita et al. (1999), Gaucher et al. (2004b, double asterisks) and this work (single asterisk). Trace fossils according to Sprechmann et al. (2004). BNFm: Barriga Negra Formation, C Esp.: Cerro Espuelitas Formation, CSFFm: Cerros San Francisco Formation, CVFm: Cerro Victoria Formation.

(Gaucher, 2000; Fig. 3). These data are in accordance with an upper Ediacaran age for the lower–middle ASG, especially considering the absence of large sphaeromorphs and acanthomorphs (Vidal and Moczydlowska-Vidal, 1997; Knoll, 2000; Grey et al., 2003).

The Cerro Victoria Formation has been placed in the lowermost Cambrian using the following criteria:

(a) Occurrence of large ichnofossils representing complex infaunal burrow systems, classified by Sprechmann et al. (2004) as *Thalassinoides* isp. This behavioural pattern is absent in the Proterozoic (Crimes, 1992). They are associated to other ichnofossils (*Planolites*, *Gyrolithes*) whose ichnofabrics follow the characteristic lowermost Cambrian pattern (Droser et al., 2002). Oldest *Thalassinoides* so far reported were assigned to the Atdabanian by Droser and Bottjer (1988). *Thalassinoides* showing almost identical preservation and size occur in the upper La Flecha Formation in the Argentine Precordillera. The La Flecha Formation has been assigned to the Upper Cambrian (Peralta, 2000; Buggisch et al., 2003). Therefore, the trace fossil assemblage of the upper Cerro Victoria Formation provides a Lower Cambrian maximum age for the unit.

(b) The absence of *Conophyton* in subtidal stromatolitic communities (Sprechmann et al., 2004), a characteristic stromatolite morphogroup of the Proterozoic, which disappears in the Cambrian (Altermann, 1999). The low-diversity stromatolite community, formed by non-branched morphogroups, is typical for upper Ediacaran and Phanerozoic communities (Walter, 1994; Altermann, 1999; Pratt et al., 2001). Stromatolite morphology alone, however, does not provide a robust age constraint and should be used with caution.

(c) Tropical climate reported for the Cerro Victoria Formation (Montaña and Sprechmann, 1993) correlates better with the Lower Cambrian global warming (Riding, 1994).

(d) Finally, the unit is older than widespread granitic and syenitic magmatism in the Nico Pérez Terrane, ranging in age from 535 to 520 Ma (Bossi and Campal, 1992; Kawashita et al., 1999). Furthermore, a granitic mylonite from a shear zone affecting the Cerros San Francisco and Cerro

Victoria Formations (Fig. 2) yielded a Rb–Sr age of 540±25 Ma (Umpierre and Halpern, in Bossi and Campal, 1992). These datings show that minimum age of the Cerro Victoria Formation is Lower to Middle Cambrian.

Gaucher (2000) reported the occurrence of a few, poorly-preserved specimens of *Lophosphaeridium montañae* and *Myxococcoides* sp. from dolostones belonging to the Cerro Victoria Formation. We prepared five palynologic macerations of stromatolitic and micritic, medium-gray dolostones of units B, C and D, which were found to be barren. Therefore, no biostratigraphic inferences can be done based on the available organic-walled microfossils.

Hence, according to the data summarized above, deposition of the Cerro Victoria Formation most probably took place in the Nemakit–Daldyn stage (Brasier et al.,

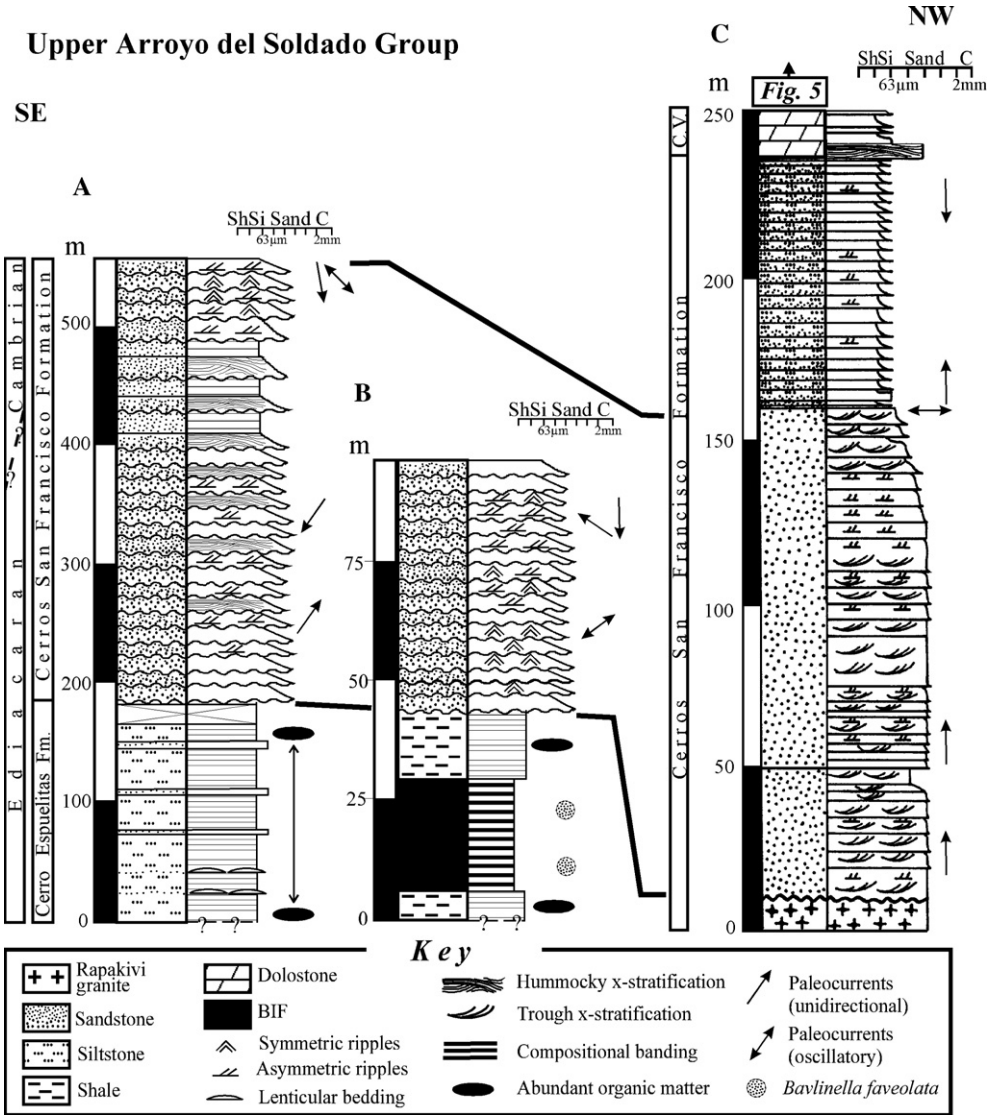

Fig. 4. Lithostratigraphic correlation of key sections of the upper Arroyo del Soldado Group (see Fig. 1 for location). A: Cerro de la Sepultura section (Gaucher, 2000: text-fig. 27), B: Cerro Magnético section (Gaucher, 2000: text-fig. 24), C: Arroyo de la Pedrera Syncline (Fig. 2), modified from Montaña and Sprechmann (1993). Distance between sections: A–B: 17 km, B–C: 70 km. CV: Cerro Victoria Formation. Thickness of the Cerros San Francisco Formation increases toward the east. At the same time, its basal erosional unconformity is more deeply incised toward the west. Due to the present erosional level, carbonates of the Cerro Victoria Formation are only preserved in the west (section C). Total organic carbon values (TOC) observed for organic-rich shales of the Cerro Espuelitas Formation (sections A–B) reach maximum values of 11% TOC. Fig. 5 is the continuation of the stratigraphic column shown in C.

1994), and a slightly younger age (Tommotian–Atdabanian) for the *Thalassinoides*-bearing carbonates is allowed by the error bars of the above mentioned datings. Chemostratigrapic data presented below support a Lower Cambrian age assignment.

3. Lithostratigraphy of the Cerro Victoria Formation

Montaña and Sprechmann (1993) were the first to recognize the existence of stromatolitic communities in Uruguay, which were discovered in the Cerro Victoria Member. Gaucher et al. (1996) gave this unit the rank of a formation and include it in the Arroyo del Soldado Group. Sprechmann et al. (2004) described in detail stromatolitic communities and associated trace fossils of the Cerro Victoria Formation. The outcrop area is located approximately 8 km NW of the town of Illescas, in the Florida Department (Figs. 1 and 2). The unit conformably overlies quartzarenite of the Cerros San Francisco Formation, which is a laterally extensive unit in the Arroyo del Soldado basin (Gaucher and Schipilov, 1993; Gaucher, 2000). The contact of the Cerro Victoria Formation with the underlying Cerros San Francisco Formation is transitional, as observed in the Arroyo de la Pedrera section (Fig. 5). The Cerros San Francisco Formation overlies with erosional unconformity the Cerro Espuelitas Formation (Fig. 4) or directly rests on older basement

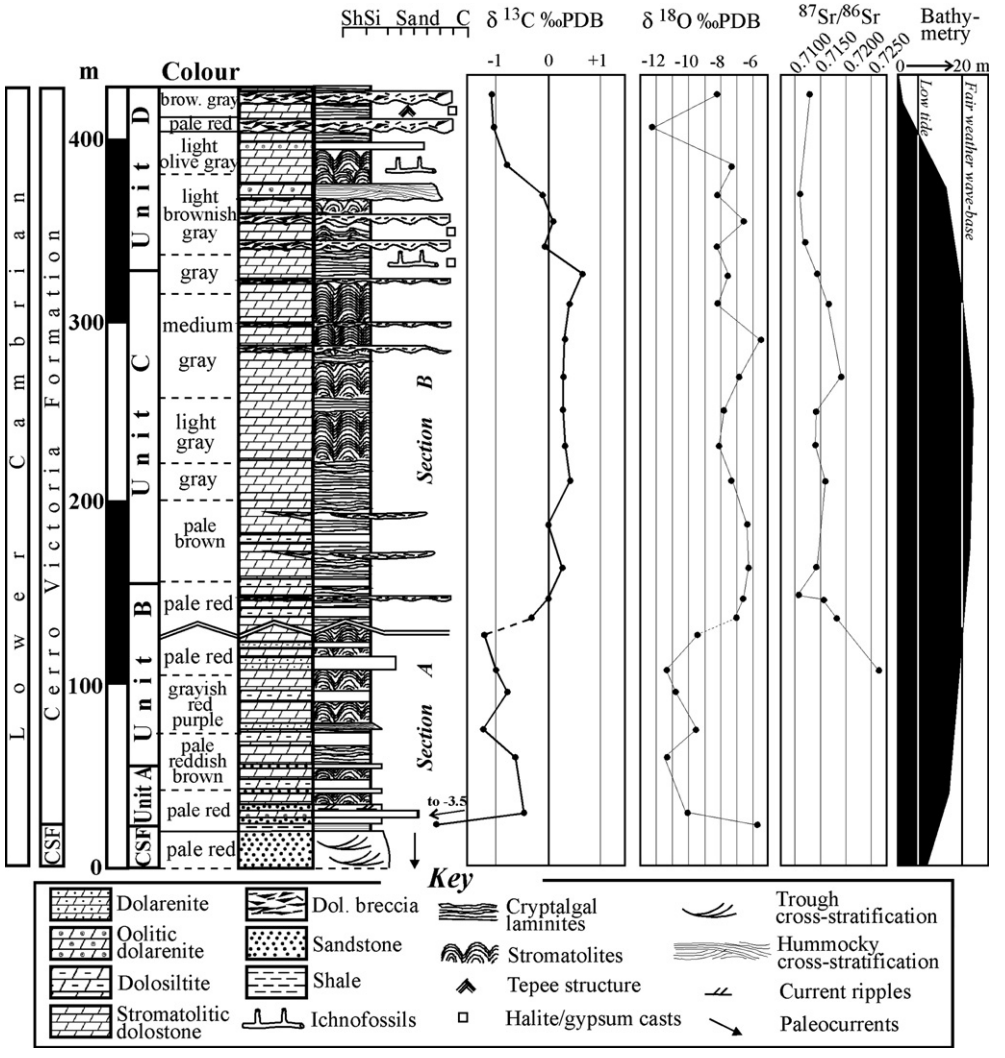

Fig. 5. Stratigraphic column of the Cerro Victoria Formation at sections A and B (Fig. 2), showing corresponding C, O and Sr-isotopic data. CSF: Cerros San Francisco Formation.

(Gaucher, 2000; Fig. 4). The only area observed so far where carbonates of the Cerro Victoria Formation have been preserved is its type area (Figs. 2, 5), located in the western (shallower) part of the Arroyo del Soldado basin. In the east, the Cerros San Francisco Formation is truncated by the present erosion level (Fig. 4).

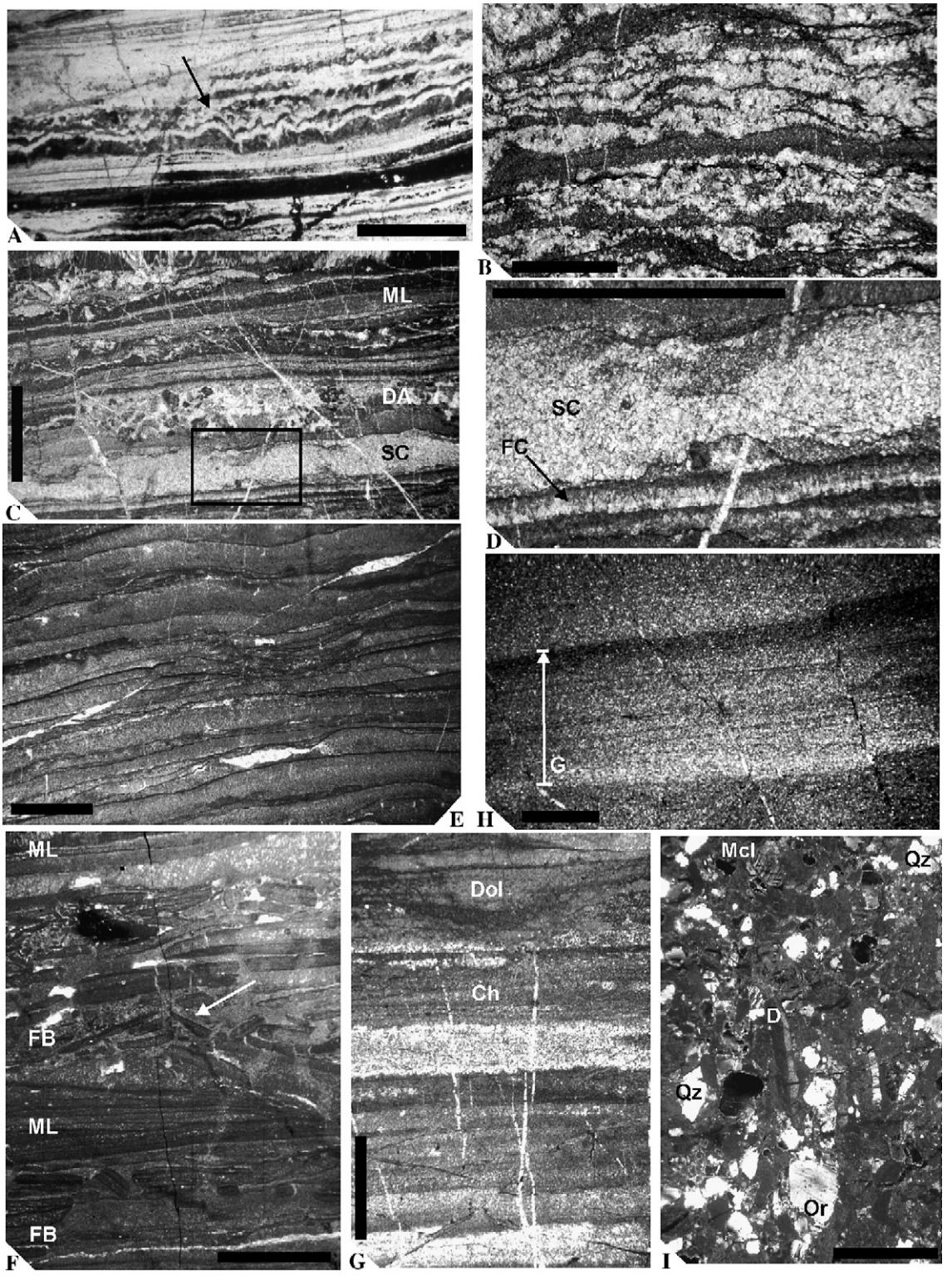

The Cerro Victoria Formation is here divided into four informal lithostratigraphic units. Contacts between the units are transitional. We recognize from base to top:

(1) Unit A. It is composed by quartzose sandstones interbedded with cm-scale dolarenite beds, characterized by a high abundance of terrigenous, notably quartz and subordinated microcline, perthitic orthoclase and plagioclase (Fig. 6I). Well-sorted ooids up to 0.6 mm in diameter are a subordinate component of the dolarenites. Domal stromatolites up to 1.6 m in diameter occur as well. Thickness of this unit reaches 30 m. Mixed carbonate–siliciclastic deposition and initial colonization of the substrate by pioneer microbial communities were the dominant sedimentary processes.

(2) Unit B. Close laterally-linked hemispheroids and subordinate planar stromatolites (Logan et al., 1964) interbedded with pale red dolosiltite beds 5–50 cm in thickness occur. Stromatolites form sheet-like bioherms up to 4 m in height. Dolosiltite beds are massive, and often contain rounded quartz clasts (Fig. 7F). Graded dolarenite–dolosiltite beds showing hummocky cross-stratification were deposited during rare storm events (Fig. 6H). Dominant sedimentary processes in this unit, which reaches 100 m in thickness, were bioherm growth periods alternating with micrite deposition from suspension.

(3) Unit C. Planar stromatolites (cryptalgal laminites) represent the dominant facies of the unit (Figs. 6E, 8B), which has a total thickness of 180 m. Short columnar and domal stromatolites up to 1 m in diameter occur, especially at the top (Figs. 6B–D, 8A). They are often elongated in a NE-direction. Subordinate stromatolitic breccias (Fig. 7H) fill small-scale, channel-like structures (Fig. 5). Organic matter is more abundant in this unit, and gives a light to medium-gray colour to the dolostone. The predominant process during deposition of this unit was sediment trapping and binding by microbial mats in a relatively low-energy environment. Stromatolite elongation is interpreted as the result of wave or tidal currents (Sprechmann et al., 2004).

(4) Unit D. The upper 100 m of the Cerro Victoria Formation are made up of an alternation of dolomitic flake breccias, stromatolitic dolostones and oolitic dolarenites. Stromatolites are mainly represented by cryptalgal laminites, small, close and spaced laterally-linked hemispheroids (maximum diameter 0.4 m; Figs. 6A, 8C-D), and occasionally microdigitate forms (Sprechmann et al., 2004). The unit is characterized by numerous dolomitic breccia beds up to 1 m in thickness (Fig. 7G), which are interbedded with stromatolitic dolostones described above. They consist of cm-scale, subangular to subrounded stromatolite and dolosiltite clasts, which present tangential contacts or float in a dolosiltitic–dolarenitic matrix (Fig. 7G–H). Fine to coarse dolarenites are also common in the unit, and form beds 5–100 cm in thickness. Some dolarenite beds are exclusively composed of well-sorted, dolomitic ooids and stromatolite fragments (Fig. 7B), ooids showing well preserved, tangential (Fig. 7D–E) and radial structure (Fig. 7A–C). Hummocky cross-stratification occurring in these beds, shows that they represent storm deposits. Occasional halite, gypsum pseudomorphs and tepee structures have been reported by Montaña and Sprechmann (1993) and Sprechmann et al. (2004), indicating periods of subaerial exposure and hypersaline conditions. Trace fossils were described and illustrated by Sprechmann et al. (2004) from this unit, which were assigned to the ichnogenera *Thalassinoides*, *Planolites* and *Gyrolithes*. Apart from the occurrences at the type area (Fig. 2, section C), we found trace fossils at the same stratigraphic level in the Arroyo de la Pedrera section (Fig. 2, section B). Pervasive early silicification affects the burrows, but also the stromatolitic and oolitic dolostones of the upper part of the unit (Figs. 6G, 7D–E, 8C), which might be related to hypersaline conditions. High energy processes were dominant during

Fig. 6. Stromatolitic and clastic dolostones of the Cerro Victoria Formation. (A) Silicified stromatolitic dolostone of unit D showing early botroydal cements (arrowed). (B) Stromatolitic dolostone of unit C, made up of an alternation of dolomicritic laminae (dark) and early microdolosparitic cements. (C) Stromatolitic dolostone of unit C, composed of alternated microbial laminations (ML), dolarenite (DA) and dolosparitic cements (SC). (D) Enlargement of area indicated in (C), showing early dolosparitic (SC) and fibrous (FC) cements. (E) Cryptalgal laminites (planar stromatolites) composed of very fine-grained dolomite, uppermost unit B. (F) Interbedded microbial laminations (ML) and flake breccias (FB), uppermost unit B. Note possible tepee structure (arrowed). (G) Silicified cryptalgal laminites of the uppermost unit D, crossed nicols. Note fine-grained chert (Ch) and dolosiltite relics (Dol). (H) Normally graded laminae (dolarenite–dolosiltite) of unit A, showing hummocky cross-stratification at the outcrop level. (I) Impure dolarenite from the Cerros San Francisco–Cerro Victoria transition, crossed nicols (bedding plane is vertically oriented). Note dolosiltite clasts (D), but also abundant terrigenous (quartz, microcline, orthoclase). Scale bars represent 2.5 mm for all figures.

deposition of unit D, as shown by stromatolitic flake breccias and cross-bedded, oolitic dolarenites. High evaporation rates and occasional subaerial exposure are indicated by tepee structures, disseminated evaporites (Sprechmann et al., 2004) and early silicification.

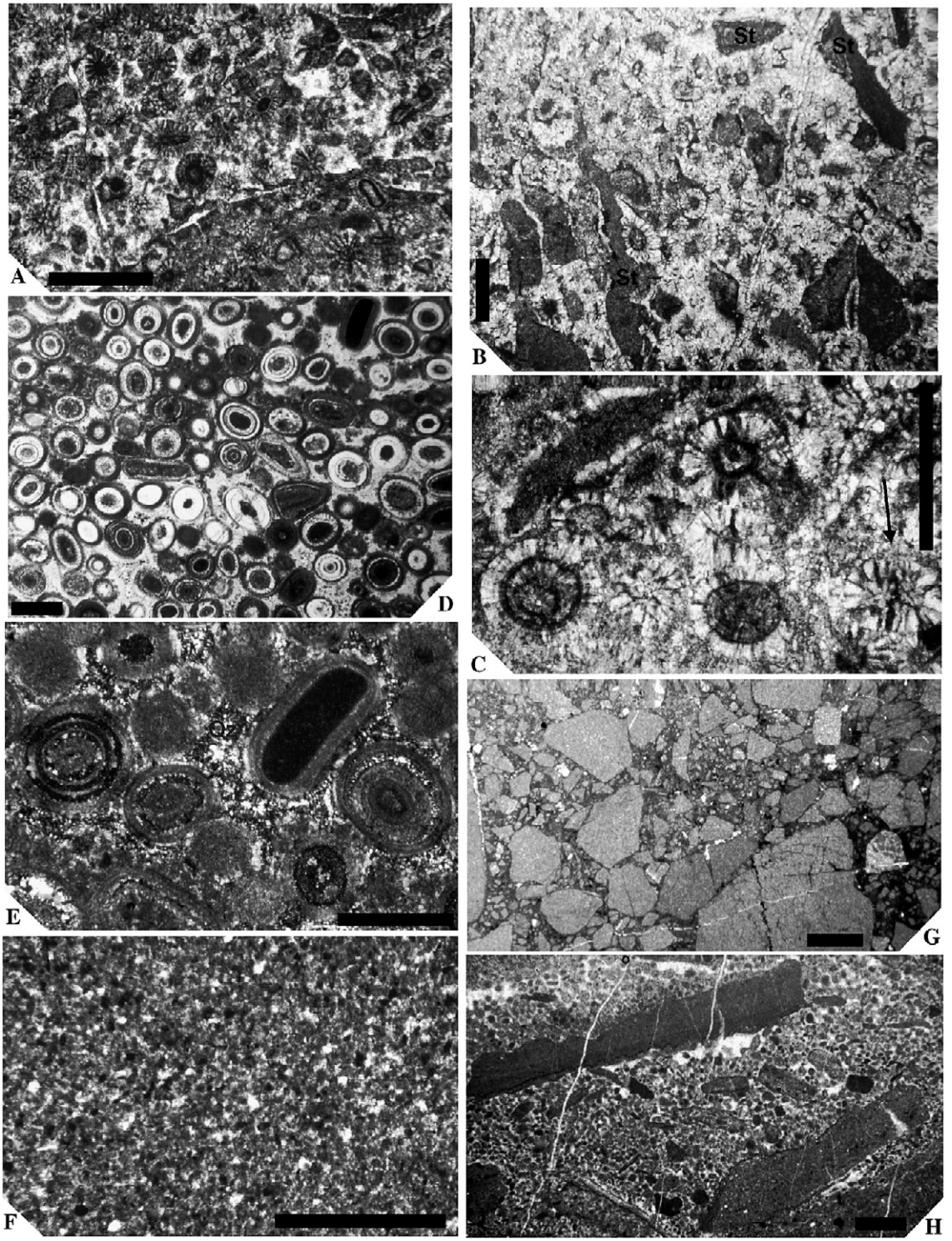

Colour of dolostone is consistently pale red to purple red (10R 6/2 to 5RP 4/2) at the base of the Cerro Victoria Formation, light to medium gray (N7 to N5) in the middle and light brownish gray (5YR 6/1) at the top, representing a useful stratigraphic criterium (Fig. 5). Whereas reddish and brownish colours are determined by disseminated, fine-grained hematite, gray colours are due to a higher organic matter content, as shown by the amount of organic matter recovered in acid macerations of these rocks. This shows that well-oxygenated sedimentary environments at the base and top of the Cerro Victoria Formation are separated by a period of oxygen-deficient (but not anoxic) bottom waters at the middle of the unit.

4. Materials and methods

Standard thin sections of carbonates were prepared, stained (Alizarin Red-S) and carefully analyzed under a petrographic microscope Leica DM LP. Domains consisting of pure primary carbonates and showing no recrystallization were selected. Approximately 1 g of these domains was extracted from the corresponding rock specimen. Least altered samples (lacking veins, discoloration, weathered rinds, recrystallization features, and silicification) were microdrilled with 1 mm drill at the LABISE, Federal University of Pernambuco, Brazil. CO_2 was extracted from these carbonate samples in a high vacuum line after reaction with phosphoric acid at 25 °C (12 h of reaction for limestones or 3 days for dolostones), and cryogenically cleaned, according to the method described by Craig (1957). CO_2 gas released was analyzed for O and C isotopes in a double inlet, triple collector mass spectrometer (VG Isotech SIRA II), using the BSC reference gas (Borborema skarn calcite) that calibrated against NBS-18 (carbonatite), NBS-19 (toilet seat limestone) and NBS-20 (Solenhofen limestone), has a $\delta^{18}O$ value of $-11.3‰_{PDB}$ and $\delta^{13}C = -8.6‰_{PDB}$. The external precision based on multiple standard measurements of NBS-19 was better than 0.1‰ for carbon and oxygen. The results are expressed in the δ-notation in parts per thousand in relation to international PDB scale. Samples chosen for Sr-isotopic analyses were leached in 0.5 M acetic acid and centrifuged to separate the dissolved and insoluble fractions. Sr was eluted from solutions by ion exchange chromatography using Sr-Spec resin. $^{87}Sr/^{86}Sr$ values were determined in static mode using a Finnigan MAT 262 seven-collector mass spectrometer at the University of Brasilia, Brazil. The isotopic ratios were normalized to $^{86}Sr/^{88}$ Sr value of 0.1194 and the 2σ uncertainties on Sr-isotope measurements was less than 0.00017, except for two samples (030130/8 and 10, Table 1) with $2\sigma = 0.00037$. Repeated analyses of NIST 987 standard over the analysis period indicated a value of 0.71028 + 0.00002 (2 σ) for the $^{87}Sr/^{86}Sr$ ratio. Whole-rock chemical analyses were carried out on fused beads by XRF at the LABISE, Recife. Palynological macerations of carbonates and pelites were prepared at the Micropalaeontology Laboratory of the Facultad de Ciencias (Montevideo). Following crushing and digestion of samples (ca. 150 g) with concentrated HCl, 72% HF was applied for 24 h to the silicate/organic residues. After neutralization, boiling, concentrated HCl was used to dissolve fluorides. Remaining organic residues were recovered by means of a 5 μm sieve, stored in glass flasks and mounted with glycerin-gelatine on standard glass slides. Organic matter abundance was semi-quantitatively estimated during this stage.

5. Chemostratigraphy

5.1. Sections studied

We sampled continuous sections of the Cerro Victoria Formation at its stratotype, located along the Arroyo de la Pedrera (sections A and B, Fig. 2). There, the transition between the Cerros San Francisco and Cerro Victoria Formations is well exposed, as well as the overlying carbonates (Fig. 5). To avoid stratigraphic repetition due to parasitic folds, two separate sections were sampled (Fig. 2). However, fitting of both sections could be easily achieved, because distinctive lithologies of unit B occur at the top of section A and at the base of section B (Fig. 5). Finally, a short parallel section located at the top of the Cerro Victoria hill (Fig. 2, section C) was sampled, where common trace fossils occur.

C- and O-isotope data show smooth, low-amplitude secular oscillations which are roughly coincident with

Fig. 7. Oolitic and clastic dolostones of the Cerro Victoria Formation. (A) Oolitic dolarenite of unit D at section B (Fig. 5). Note predominantly radial structure of ooids. (B) The same bed as the previous, but at section C (Fig. 9). Note common stromatolitic fragments (St) and ooids (bedding plane is vertically oriented). At the outcrop level, hummocky cross-stratification is evident. (C) Close up of dolomitic ooids of the previous figure, showing both tangential and radial structure, as well as one ooid with two nuclei (arrowed). (D) Oolitic dolarenite of unit D characterized by an early siliceous cementation that prevented compaction of ooids. (E) Enlargement of ooids of the previous sample, crossed nicols. Note tangential structure of ooids and elongate ooid nucleated around a stromatolite fragment. (F) Typical texture of medium to coarse dolosiltite, containing rounded terrigenous clasts. Upper unit B. (G) Intraclastic breccia composed of angular dolosiltite clasts cemented by dolomite and hematite, unit D. (H) Flake breccia made up of stromatolite fragments in a dolarenitic matrix, unit C. Scale bars represent 1 mm for all figures.

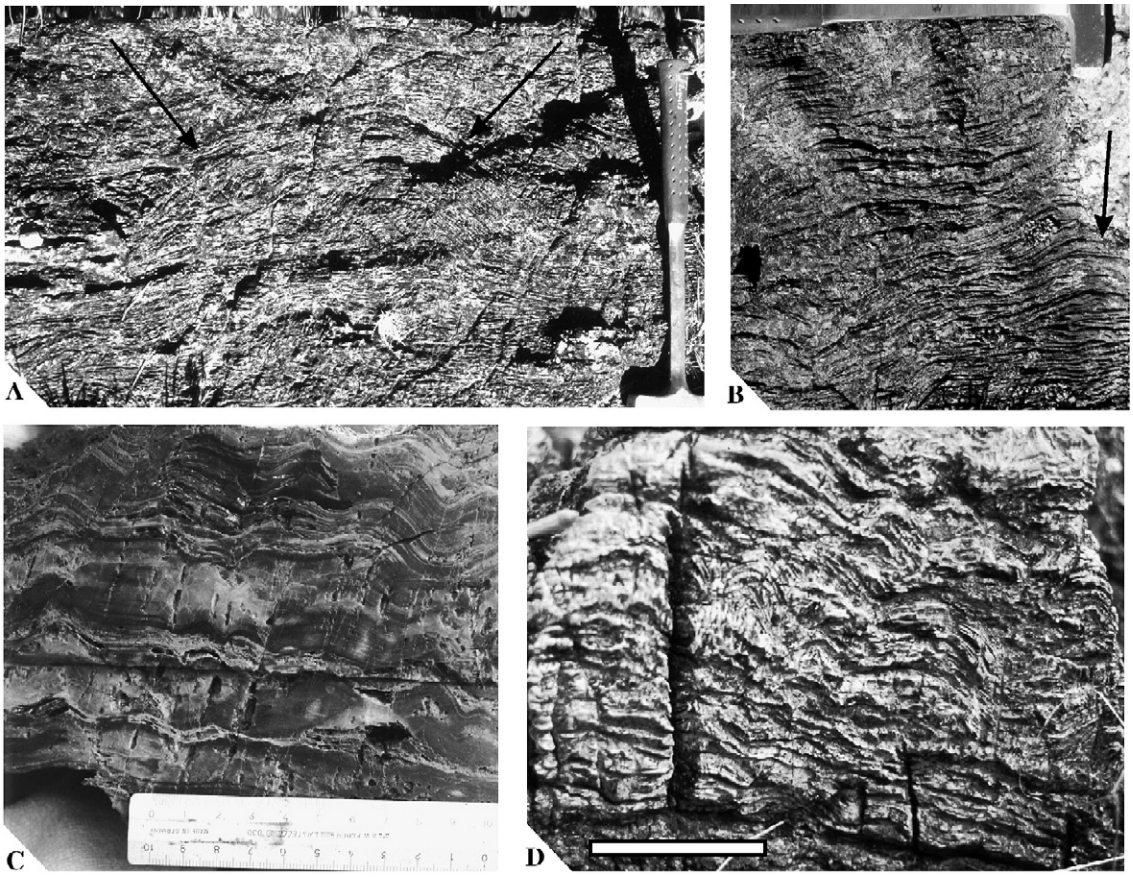

Fig. 8. Stromatolites of the Cerro Victoria Formation. (A) Domal stromatolite 50 cm in diameter (arrowed), unit C. Length of hammer: 40 cm (B) Planar and small domal stromatolites (arrowed), upper unit C. Trace fossils occur above this lithology in section A–B (Fig. 5). (C) Silicified stromatolites, upper unit D. (D) Small, laterally-linked hemispheroids occurring at the transition between units C and D. Scale bar measures 10 cm.

facies changes. We are confident that sections A and B are contiguous, as shown by litho- and chemostratigraphic data (Fig. 5). On the other hand, section C matches carbonates from section AB between 320 and 360 m (Figs. 5, 9). Apart from the same C- and O-isotope values, a thick oolitic marker bed and immediately underlying trace fossils in both sections allow a confident correlation.

5.2. Carbon and oxygen isotopes

A negative $\delta^{13}C$ interval is recorded at the Cerros San Francisco–Cerro Victoria transition (Fig. 5). One sample from stromatolitic dolostones occurring at the contact at point D (Fig. 2) yielded the most negative values of $-3.5‰_{PDB}$ (Boggiani, 1998; Gaucher, 2000). Up section, values remain negative throughout units A and B, reaching a plateau around -1.0 to $-1.3‰_{PDB}$. After ca. 130 m of carbonates yielding negative $\delta^{13}C$ values, positive values around $+0.3‰_{PDB}$ are recorded at the transition between units B and C (Fig. 5). This positive excursion shows fairly constant values for ca. 180 m of mainly stromatolitic carbonates of unit C (Fig. 5). Peak $\delta^{13}C$ values occur at the top of unit C, yielding $+0.64‰_{PDB}$. Up section (lower unit D), very low-amplitude, short wavelength oscillations around a mean value of $0‰_{PDB}$ are recorded in trace fossil-bearing dolostones both at sections B and C. Finally, increasingly negative values of up to $-1.1‰_{PDB}$ characterize uppermost carbonates of the Cerro Victoria Formation, concomitant to an increase in the frequency and thickness of intercalated intraformational breccias.

$\delta^{13}C$ values in most of the analyses reported here represent primary or near-primary isotopic ratios, because:

(a) $\delta^{13}C$ values in the sections studied vary smoothly and independently from lithologies sampled,
(b) We carried out 4 analyses of closely spaced samples (0.8 m) representing two stromatolitic

Table 1
Isotopic composition, Mn and Sr concentration of Cerro Victoria dolostones

Sample	Section	Description	$\delta^{18}O$ ‰ PDB	$\delta^{13}C$ ‰ PDB	$^{87}Sr/^{86}Sr$	Mn (ppm)	Sr (ppm)
ILL 2A*	D	Stromatolitic dolostone	−5.70	−3.48			
030130/1	A	Impure dolarenite, ooids	−10.21	−0.45			
030130/2	A	Thrombolitic dolosiltite	−11.54	−0.66			
030130/3	A	Graded, impure dolosiltite	−9.48	−1.27		492	135
030130/4	A	Fine, massive dolosiltite	−10.86	−0.77			
030130/5	A	Impure dolosiltite	−11.29	−1.03	0.72644		
030130/7	A	Microsparitic dolostone	−9.43	−1.21			
030130/8	B	Cryptalgal laminites, dolost.	−7.10	−0.29	0.71825		
030130/9A	B	Cryptalgal laminites, dolost.	−5.10	0.31	0.71535		
030130/9B	B	Fine, massive dolosiltite	−8.56	−0.13	0.71064		
030130/9C	B	Cryptalgal laminites–flake breccia	−6.92	−0.02			
030130/9D	B	Dolosiltite–intraformational breccia	−5.87	−0.08		364	79
030130/10	B	Cryptalgal laminites–dolarenite	−6.19	0.24	0.71471		
030130/11	B	Cryptalgal laminites, dolost.	−6.36	0.03			
030130/12	B	Stromatolitic dolostone	−7.20	0.43	0.71595		
030130/13	B	Stromatolitic dolostone	−8.11	0.29	0.71408		
030130/14	B	Dolosiltite, microbial lamin.	−7.71	0.25	0.71422		
030130/15	B	Cryptalgal laminites, dolost.	−6.77	0.27	0.71925		
030130/16	B	Dolomitic flake breccia	−5.54	0.30		172	74
030130/17	B	Stromatolitic dolostone–flake breccia alternation	−8.22	0.41	0.71636		
030130/18	B	Stromatolitic dolostone	−7.53	0.64	0.71424		
030130/19	B	Dolomitic flake breccia	−8.20	−0.06			
030130/20	B	Dolosiltite–dolarenite	−6.54	0.08			
030130/21	B	Oolitic dolarenite	−8.26	−0.13			
030130/22	B	Fine dolarenite	−7.23	−0.79		138	58
030130/23	B	Dolomitic intrafor. Breccia	−12.27	−1.06			
030130/24	B	Cryptalgal laminites, dolostone, silicified	−8.22	−1.08	0.71302		
030130/25	C	Oolitic dolarenite	−6.39	−0.12	0.71094		
030130/26	C	Dolosiltite, microbial lamin.	−6.44	0.24			
030130/27	C	Dolomitic flake breccia	−5.69	−0.24	0.71168		
030130/28	C	Dolarenite–dolosiltite	−6.45	−0.25			

Sample marked with an asterisk from Boggiani (1998).

dolostone beds and two dolosiltite beds (samples 030130/9, Table 1). Whereas $\delta^{13}C$ values obtained are consistent (+0.31,−0.13,−0.02 and −0.08‰$_{PDB}$), $^{87}Sr/^{86}Sr$ values obtained for the lower two samples, a stromatolitic dolostone and a dolosiltite, differ markedly (0.71535 and 0.71064 respectively, Table 1). This suggests that whereas Sr-isotopic values were significantly affected by diagenesis, C-isotopic values reflect near-seawater composition.

(c) Parallel section C, which was correlated with section B based on lithostratigraphy and fossils

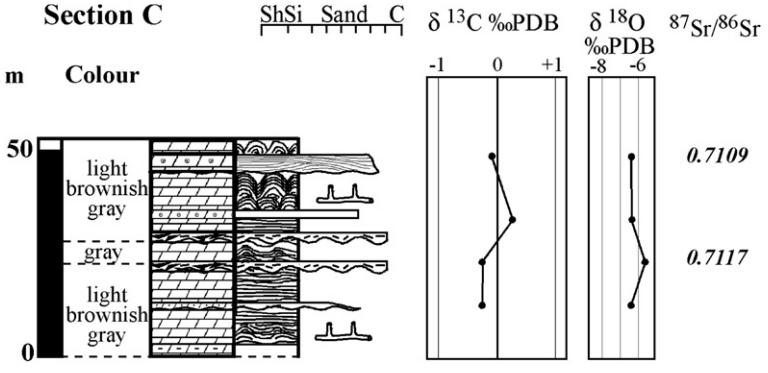

Fig. 9. Cerro Victoria hill section (Fig. 2, section C). This section matches carbonates in the 320–360 m interval of section A–B (Fig. 5). Key: see Fig. 5.

(see chapter 5.1), yielded C-isotopic compositions indistinguishable from the correlative dolostones of section B.

(d) Dolostones yielded $\delta^{18}O$ values mostly (84%) above −10‰$_{PDB}$, suggesting that $\delta^{13}C$ determinations reflect near-seawater composition (Derry et al., 1994; Corsetti and Kaufman, 1994; Jacobsen and Kaufman, 1999). Only five $\delta^{18}O$ determinations range between −10.2 and −12.3‰$_{PDB}$.

Limestone alteration proxies, such as Mn/Sr, Fe/Sr and Sr concentration, should not be applied without further considerations to dolostones, since chemistry and structure of dolomite allows less amounts of Sr to be incorporated into the lattice, but far more Fe and Mn (Deer et al., 1992; Kah et al., 1999). Furthermore, Fe and Mn can replace for Mg during diagenesis (Tucker, 1990a) but also during deposition of primary dolomites formed in reducing conditions (Vasconcelos and McKenzie, 1997; Gaucher, 2000), so that high Mn/Sr and Fe/Sr values do not necessarily reflect diagenetic alteration. Gaucher et al. (2003) reported that isotopic composition of co-occurring calcarenite and dolosiltite laminae from rhythmites of the uppermost Polanco Formation (sample 980317/7, Gaucher et al., 2003: Table 1) differ only by 0.3‰ ($\delta^{13}C$) and 0.9‰$_{PDB}$ ($\delta^{18}O$). Thus, dolomite evidently reflects seawater isotopic composition in this example. Corsetti and Kaufman (1994) interpreted $\delta^{13}C$ profiles from Neoproterozoic–Cambrian dolostones of western United States as primary in nature, despite high Mn/Sr (>3) and low $\delta^{18}O$ values (<−11‰). Bekker et al. (2003) suggest that high Fe/Sr and Mn/Sr values found in Palaeoproterozoic dolostones from the Minas Supergroup (Brazil) do not imply diagenetic alteration, since Archean and early Paleoproterozoic dolomites are known to contain more Fe and Mn than Phanerozoic carbonates. Kah et al. (1999) conclude that carbon isotopic composition of dolostones of the Mesoproterozoic Bylot Supergroup of Canada primarily reflects variations in seawater composition, despite high Mn/Sr ratios.

5.3. Strontium isotopes

The strontium isotopic record of the Cerro Victoria Formation is ambiguous and difficult to interpret. $^{87}Sr/^{86}Sr$ values are too radiogenic throughout the unit to reflect seawater composition, with a mean around 0.7150. The lowest values were found in the basal part of unit C (0.7106) and in oolitic dolarenites of unit D (0.7109). These, however, are ca. 0.0012 higher than the highest $^{87}Sr/^{86}Sr$ near-seawater values so far reported, which occur in Upper Cambrian carbonates (0.7094: Montañez et al., 2000; Fig. 10B). Thus, two explanations

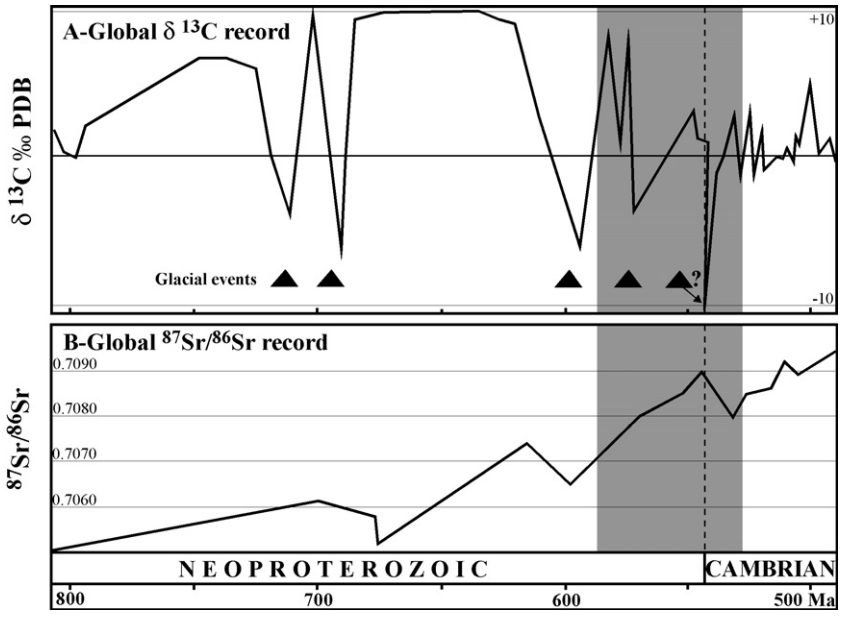

Fig. 10. Neoproterozoic to Cambrian strontium and carbon-isotopic composition of marine carbonates, showing the interval represented by the Arroyo del Soldado Group (shaded area). (A) Global late Neoproterozoic–Cambrian $\delta^{13}C$ curve. Neoproterozoic part of the curve mainly according to Walter et al. (2000) and Jacobsen and Kaufman (1999), and Cambrian isotopic record according to Brasier and Sukhov (1998) and Montañez et al. (2000). (B) Sr-isotopic record of Neoproterozoic–Cambrian seawater composition, according to Melezhik et al. (2001, and references therein) and Montañez et al. (2000). Note indentations of the curve at ca. 675, 600 and 535 Ma, roughly matching important rifting events.

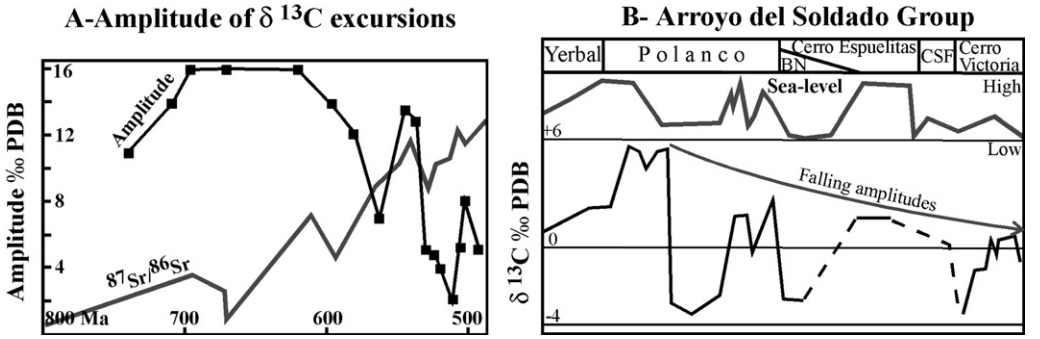

Fig. 11. Falling amplitudes of $\delta^{13}C$ oscillations in late Neoproterozoic–Cambrian carbonates, and $\delta^{13}C$ and sea-level record of the Arroyo del Soldado Group. (A) Amplitude of $\delta^{13}C$ excursions (same sources as Fig. 10A) vs. time. Strontium-isotopic curve illustrated in Fig. 10B is shown at the same scale for comparison. Increasing amplitude of isotope excursions between 750 and 700 Ma was followed by a plateau (at 16‰) and finally a sharp decrease. Low $^{87}Sr/^{86}Sr$ values characterize periods of high amplitude in $\delta^{13}C$ oscillations, progressively increasing while amplitudes fall to a minimum in the Middle Cambrian. Note unusually high amplitude of $\delta^{13}C$ excursion at the Precambrian–Cambrian boundary (542 Ma: Amthor et al., 2003). (B) Carbon-isotopic record and sea-level oscillations in the Arroyo del Soldado Group. BN: Barriga Negra Formation, CSF: Cerros San Francisco Formation. Note covariation of $\delta^{13}C$ and sea-level, and falling amplitudes of $\delta^{13}C$ positive excursions (data from Gaucher et al., 2003, 2004a, this work).

can be put forward to account for the exceedingly high $^{87}Sr/^{86}Sr$ values. First, diagenetic alteration of carbonates might account for the enrichment in radiogenic Sr. Geochemical data, such as Mn/Sr ratios between 4.6 and 2.3 and low Sr concentrations (60–80 ppm), point in this direction (Jacobsen and Kaufman, 1999; Melezhik et al., 2001), though applicability of these proxies to dolostones is problematic (see above). On the other hand, relatively high oxygen isotopic values (−7 to −8‰ in the least radiogenic samples) and an excellent textural preservation (Figs. 6 and 7) militate against this interpretation. An alternative explanation might be the influx of meteoric water (riverine or groundwater) into the basin, thus providing higher amounts of radiogenic Sr to the basin or the early diagenetic environment (Dickson, 1990; Veizer, 1994). Especially the non-stoichiometric ($Ca_{54–55}$), Ca-rich nature of dolomite is consistent with lower Mg/Ca ratio of mixing zones (Tucker, 1990a). However, even though mixing of meteoric water seems probable for the lowermost Cerro Victoria Formation (unit A), it is difficult to assume for the rest of the unit, where a strong marine influence is indicated by sedimentary structures and microfacies (see above). A combination of both–diagenetic and mixing–processes is probably responsible for the high and rather erratic $^{87}Sr/^{86}Sr$ values found in the unit.

6. Discussion

6.1. Genesis of dolomite

Previous reports did not recognize the dolomitic nature of the Cerro Victoria Formation (Montaña and Sprechmann, 1993; Gaucher, 2000; Sprechmann et al., 2004), mainly because no typical dolomitization features occur, either at the outcrop or microscopic level. Geochemistry and thin-section staining techniques applied in this work revealed that carbonates of the Cerro Victoria Formation are composed by virtually 100% dolomite. A number of petrographic features of the Cerro Victoria dolostones point to a primary or penecontemporaneous nature of the dolomite. These include:

(1) Excellent preservation of textural details of carbonates, such as ooid microstructure (Fig. 7A–E), fine dolomicrite (grainsize 5–20 μm), early fibrous and sparry cements in stromatolitic dolostones (Fig. 6A–D) and isopachous cements on dolarenite clasts and ooids (Fig. 7E). These features favor a primary origin for the dolomite (Tucker, 1982, 1990b), but it must be noted that Zempolich and Baker (1993) experimentally demonstrated that early diagenetic dolomitization is capable of preserving fine textural details similar to those observed.
(2) Non-stoichiometric nature of dolomite, which usually contains 54–55% $CaCO_3$ unlike most burial dolomites (Tucker, 1990a).
(3) Complete absence of calcite relicts and replacive textures in the dolostone at the resolution of the optical microscope.
(4) An early siliceous cementation occurs in the upper Cerro Victoria Formation (unit D), which preserved microfabric details. Carbonate relics are exclusively made up of dolomite, showing its pre-silicification origin (Figs. 6A, G; 7D–E).

Gaucher (2000) argued for the primary nature of dolomite occurring in the Polanco Formation, and

suggested that its genesis is related to bacterial sulphate reduction in an anoxic environment, according to the model proposed by Vasconcelos and McKenzie (1997). However, pyrite and important amounts of associated organic matter, widespread in the Polanco dolostones, are absent in the shallower Cerro Victoria Formation. Carbonates of unit C, deposited under oxygen-deficient conditions, are as dolomitic as carbonates from the other units, which record well-oxygenated environments. Thus, a different mechanism might have determined that dolomite is the dominant carbonate species in the Cerro Victoria Formation. The available data do not allow to rule out a very early diagenetic (i.e. penecontemporaneous) origin of dolomite. The distinction of a primary versus penecontemporaneous origin requires additional techniques (e.g. SEM and further isotopic analyses, Zempolich et al., 1988) that would be out of the scope of this paper. Tucker (1982, 1990b) suggested that a different seawater composition determined precipitation of primary dolomite in the Neoproterozoic Beck Spring Dolomite and elsewhere. According to the author, a higher Mg/Ca ratio, higher atmospheric pCO_2 and a lower sulphate concentration were responsible for dolomite precipitation. Zempolich et al. (1988), however, argue that dolomitization of the Beck Spring Dolomite took place during early surficial diagenesis. High evaporation rates with concomitant gypsum/anhydrite deposition, though of little importance in the Cerro Victoria Formation, could account for both higher Mg/Ca and lower sulphate concentration. A higher pCO_2 during deposition of the Cerro Victoria Formation is suggested by the Lower Cambrian global warming (Riding, 1994). Similarly dolomitic, shallow-water carbonate units occur in the Middle to Upper Cambrian of the Argentine Precordillera (Peralta, 2000; Sial et al., 2003; Buggisch et al., 2003), but also in a number of lowermost Cambrian units elsewhere (Yudoma Formation: Derry et al., 1994, Reed and Deep Spring Formations: Corsetti and Kaufman, 1994; Dengying Formation: Steiner, 1994). A petrographic and geochemical comparison of these lowermost Cambrian dolomitic units is needed to assess the extent (i.e. regional or global) of dolomite deposition at that time. A global peak of dolomite deposition occurred in the Neoproterozoic (Tucker, 1990b), which probably lasted into the earliest Palaeozoic. However, Burns et al. (2000 and references therein) presented global curves of dolomite deposition which show a dolomite-minimum in the Cambrian.

6.2. The Precambrian–Cambrian boundary

Strontium isotopic values for the Cerro Victoria Formation reflect significant post-depositional alteration, which renders them of little use for chemostratigraphy. Carbon isotopic data, on the other hand, reflect near-seawater composition. The $\delta^{13}C$ curve obtained for the unit is remarkable for the low amplitude of the oscillations observed, around 2‰$_{PDB}$, if we except the basal negative excursion (−3.5‰$_{PDB}$; Fig. 5). This situation contrasts with values obtained for the lower and middle Arroyo del Soldado Group, in which a series of impressive, large amplitude $\delta^{13}C$ excursions occur (Gaucher et al., 2004a; Fig. 3). $\delta^{13}C$ excursions show a persistent tendency towards smaller amplitudes up section in the ASG (Figs. 3, 11B). Falling amplitudes of $\delta^{13}C$ excursions characterize Neoproterozoic to Cambrian successions worldwide (Derry et al., 1994; Brasier and Sukhov, 1998; Montañez et al., 2000; Walter et al., 2000; Brasier and Lindsay, 2001; Figs. 10A, 11A).

An upper Ediacaran (Vendian) age (580–542 Ma) for the Yerbal, Polanco and Cerro Espuelitas Formations (Fig. 3) is indicated by biostratigraphic (see above), $^{87}Sr/^{86}Sr$ (Kawashita et al., 1999; Gaucher et al., 2004b) and $\delta^{13}C$ data (Gaucher et al., 2003, 2004a). A Lower Cambrian age for the Cerro Victoria Formation has been suggested mainly on the basis of trace fossils occurring in the unit (see above), which are the best available criteria for the location of the Precambrian–Cambrian boundary (Brasier et al., 1994). Therefore, the boundary must be located somewhere between the uppermost Cerro Espuelitas and upper Cerro Victoria Formation (Fig. 3). Gaucher (2000) suggested that the boundary might be represented by the basal Cerros San Francisco erosional unconformity (Fig. 3), as also reported for many successions around the world (Corsetti and Kaufman, 1994; Germs, 1995; Kaufman et al., 1996; Brasier and Lindsay, 2001). Carbon isotopic data presented here for the Cerro Victoria Formation strongly resemble $\delta^{13}C$ curves of lowermost Cambrian (Nemakit–Daldyn stage, Fig. 10A) carbonates in Siberia (Yudoma Formation: Derry et al., 1994; Brasier and Sukhov, 1998; Manykai Formation: Kaufman et al., 1996), Mongolia (Brasier et al., 1996), western USA (Death Valley and White-Inyo, Corsetti and Kaufman, 1994; Corsetti and Hagadorn, 2000), northwestern Canada (Narbonne et al., 1994; Kaufman et al., 1997), Oman (Amthor et al., 2003) and possibly Argentina (lower La Laja Formation: Sial et al., 2003). According to the detailed $\delta^{13}C$ curve presented by Derry et al. (1994: Fig. 5), Kaufman et al. (1996) and Brasier and Sukhov (1998) for carbonates of the Siberian craton, the Cerro Victoria Formation possibly spans the interval 542–533 Ma (Figs. 10A, 11B). It is worth noting that geochronologic constraints of the mentioned curve rely on many U–Pb zircon datings coupled with detailed

biostratigraphic data (Bowring et al., 1993; Brasier, 1996; Kaufman et al., 1996; Landing et al., 1998; Brasier and Lindsay, 2001). The Precambrian–Cambrian boundary has been recently located at 542.0±0.6 Ma, as shown by U–Pb zircon age data from ash beds of the Huqf Supergroup, Oman (Amthor et al., 2003).

Given the above interpretation of the basal Cerro Victoria negative excursion as representing the upper part of the negative anomaly W of Brasier and Lindsay (2001), recognized worldwide (Shen and Schidlowski, 2000) and dated by Amthor et al. (2003) at 542 Ma, it follows that the Precambrian/Cambrian boundary should be located at the Cerros San Francisco–Cerro Victoria transition or within the upper Cerros San Francisco Formation. These results are encouraging, because they imply that the boundary could actually be preserved in the ASG, contrary to previous suggestions that located the boundary at the basal erosional unconformity of the Cerros San Francisco Formation (Gaucher, 2000). High-resolution carbon isotope chemostratigraphy of unit A of the Cerro Victoria Formation might help resolve the shape of the negative W spike and decide where to place the Precambrian–Cambrian boundary (Figs. 10A, 11B). Ongoing micropalaeontologic research, specially in search of the Lower Cambrian Small Shelly Fauna (SSF), might also constrain biostratigraphically the exact location of the boundary.

6.3. Sedimentary environments and carbon isotopes

Montaña and Sprechmann (1993) interpreted the Cerro Victoria Formation as a shallowing-upward sequence. Although there is a general shallowing-upward trend, we recognize two cycles on the basis of stromatolite morphology (Walter, 1994), sedimentary structures and carbonate facies (Fig. 5): a deepening-upward sequence spanning the lower to middle Cerro Victoria Formation, and a subsequent shallowing-upward sequence in the middle–upper part of the unit. Cryptalgal laminites and domal stromatolites of unit C represent a maximum flooding surface, which reached subtidal conditions below fairweather wave-base, occasionally affected by storms. At the same time, this interval yielded positive $\delta^{13}C$ values and higher organic matter contents (as shown by acid macerations), which determine a light to medium-gray colour of dolostone. The $\delta^{13}C$ and palaeobathymetry curves (Fig. 5) are essentially parallel throughout the Cerro Victoria Formation. Whereas periods of high sea-level are characterized by positive $\delta^{13}C$ values, carbonates deposited during regressions are ^{13}C-depleted. The same trend has been reported for the upper Ediacaran Yerbal, Polanco and Barriga Negra Formations of the ASG by Gaucher et al. (2004a; Fig. 11B). In the lowermost Cambrian, however, cycles are characterized by a much smaller amplitude of both sea-level and $\delta^{13}C$ oscillations. Gaucher et al. (2004a) reported $\delta^{13}C$ oscillations for the Polanco Formation of up to 9‰$_{PDB}$ in amplitude, and estimated the magnitude of associated sea-level oscillations in 50–100 m, on the basis of sedimentary structures. On the other hand, amplitude of $\delta^{13}C$ fluctuations in the Cerro Victoria Formation is 4‰$_{PDB}$ at most, and sea-level changes are estimated as less than 20–30 m. Buggisch et al. (2003) found the same relationship between $\delta^{13}C$ and sea-level oscillations in Middle Cambrian to Lower Ordovician carbonate successions of the Argentine Precordillera. The mentioned authors explain the coupled $\delta^{13}C$/sea-level fluctuations as a result of changing partitions between marine organic carbon and carbonate–carbon deposition. Climate changes affecting continental weathering and nutrient supply by rivers probably affected the net organic carbon burial (Buggisch et al., 2003) and caused the changing organic carbon–carbonate partitions. A younger analogy of this process has been reported by Weissert et al. (1998) for the Lower Cretaceous of the Tethyan realm. Climatic causes were also put forward to explain the coupled $\delta^{13}C$/bioproductivity/sea-level oscillations recorded in the lower Arroyo del Soldado Group (Gaucher et al., 2004a).

It is here proposed that the climatic instability characteristic of the Neoproterozoic, showing abundant evidence of global or near-global glaciation (Kaufman et al., 1997; Hoffman et al., 1998; Hoffman and Schrag, 2002), did not end abruptly at the Ediacaran/Cambrian boundary, but progressively faded away well into the Palaeozoic, as suggested by the decreasing amplitude of $\delta^{13}C$ and sea-level oscillations (Fig. 11). Change from a highly unstable Neoproterozoic global climate into a relatively stable Cambrian environment was probably due to the progressive exhaustion of nutrients pumped into the ocean during the rifting of Rodinia (Gaucher et al., 2003, 2004a), which consisted of multiple rifting events spanning the period 800–550 Ma (Gaucher and Germs, 2002; Lund et al., 2003). This is best shown by extremely low $^{87}Sr/^{86}Sr$ seawater ratios by 800 Ma (Fig. 10B), followed by steadily increasing values until the Upper Cambrian (Derry et al., 1994; Jacobsen and Kaufman, 1999; Montañez et al., 2000; Walter et al., 2000; Melezhik et al., 2001; Fig. 10). Interesting enough, the $^{87}Sr/^{86}Sr$ global curve presented in Fig. 10 is punctuated by at least three events at ca. 675, 600 and 535 Ma, during which seawater Sr-isotopic ratios were lowered by ca. 0.0010. These excursions roughly coincide with important rifting events, recognized in southern Africa, Laurentia and South America (Gaucher and Germs, 2002; Lund et al., 2003). High amounts of reductants (and nutrients) entered

the hydrosphere during low $^{87}Sr/^{86}Sr$ periods and probably determined large productivity bursts (positive $\delta^{13}C$ excursions), punctuated by severe glacial events (negative $\delta^{13}C$ excursions). The mentioned nutrients include silica, iron, manganese, phosphorous recycled from the sediments under resulting anoxic conditions (Ryding and Rast, 1989), nitrogen and a number of other micronutrients. While $^{87}Sr/^{86}Sr$ ratios rose, reflecting declining hydrothermal activity and reductant input into the ocean, both net organic carbon burial and amplitude of $\delta^{13}C$ oscillations decreased toward the end of the Neoproterozoic and into the Cambrian (Fig. 11A). At the same time, climatic instabilities and related sea-level oscillations caused by perturbations in the carbon cycle, faded away. This has profound implications for our understanding of the Cambrian evolutionary radiation of metazoans, confirming that it was strongly influenced by environmental factors (Knoll, 1994; Fedonkin, 2003).

7. Conclusions

The Cerro Victoria Formation is divided into four informal lithostratigraphic units, which are mainly composed of an alternation of stromatolitic, oolitic and clastic dolostones. Dolomite is here considered as a primary or penecontemporaneous precipitate because of excellent preservation of textural details, including early cements, ooids and dolomicrite. Data presented in this study suggest partial resetting of chemostratigraphic signals. Whereas $^{87}Sr/^{86}Sr$ ratios in the least altered samples are too high (0.7106–0.7109) to represent seawater values, $\delta^{13}C$ determinations are interpreted as reflecting near-seawater composition. The curve obtained for the Cerro Victoria Formation is characterized by low amplitude of $\delta^{13}C$ excursions. It parallels curves reported for the Nemakit–Daldyn stage of the Lower Cambrian. Considering the detailed carbon-isotopic data from Lower Cambrian carbonates of Siberia (Derry et al., 1994; Kaufman et al., 1996; Brasier and Sukhov, 1998), the Cerro Victoria Formation was probably deposited in the Nemakit–Daldyn stage, between 542–533 Ma, but we cannot definitely rule out a younger age (Tommotian–Atdabanian) for the top of the unit. In South America, carbonates of the lowermost La Laja Formation (Argentine Precordillera) show similar $\delta^{13}C$ values. On the basis of the above mentioned data, we suggest that the Precambrian/Cambrian boundary is located at the Cerros San Francisco–Cerro Victoria transition or slightly lower in the succession.

In the Arroyo del Soldado Group, $\delta^{13}C$ excursions parallel sea-level oscillations, transgressive events being characterized by positive $\delta^{13}C$ values. Falling amplitudes of coupled $\delta^{13}C$/sea-level fluctuations recorded in these carbonates are in accordance with the trend observed in Ediacaran–Lower Cambrian successions worldwide. Covariance of $\delta^{13}C$ and sea-level might be explained by bioproductivity fluctuations affecting the carbon cycle, atmospheric CO_2 concentrations, climate, ice-volume and ultimately sea-level. While these oscillations were of large magnitude in the late Neoproterozoic, they progressively faded away in the Cambrian, giving place to a more stable environment. The cause of the amplitude decrease in biogeochemical, climatic and sea-level perturbations might be the decreasing rates of nutrient (Fe, Mn, Si) input at mid-ocean ridges and consequent nutrient recycling (P, N), as reflected by rising $^{87}Sr/^{86}Sr$ values between 800 and 500 Ma. The $^{87}Sr/^{86}Sr$ curve is punctuated by at least three events at ca. 675, 600 and 535 Ma, during which seawater Sr-isotopic ratios were lowered by ca. 0.0010. These excursions roughly coincide with important rifting events, recognized in southern Africa, Laurentia and South America, providing an explanation for the long-lasting impact on the biosphere. Therefore, tectonics is envisaged as the ultimate driving force behind long-term climate change. Finally, climate amelioration probably promoted the explosive diversification of animals in the Lower Cambrian.

Acknowledgements

This study is part of a project financed by PROSUL/CNPq (project AC-38/2002) involving researchers from Brazil, Argentina, Chile and Uruguay. Funding was also provided by research project CONICYT 6007, a CSIC grant to C.G. and a CSIC-VSP project ("Litoestratigrafía, petrografía y edad del Grupo Mina Verdún"). We thank Miguel Parada, Alejandro Tosselli and Gonzalo Blanco for invaluable help during field work in Uruguay. Constructive and insightful reviews by A.J. Kaufman, Y. Shen and an anonymous reviewer are gratefully acknowledged. This is a contribution to IGCP project 478 "Neoproterozoic–Early Palaeozoic Events in SW-Gondwana" and the NEG-LABISE contribution n. 238.

References

Altermann, W., 1999. Die Sedimente der Transvaal Supergruppe, Kaapvaal Kraton, Südafrika: Stromatolithenfazies, Beckenanalyse und regionale Entwicklung im Neoarchaikum und Paläoproterozoikum. Münchner Geol. Hefte A 25, 1–140.

Amthor, J.E., Grotzinger, J.P., Schröder, S., Bowring, S.A., Ramezani, J., Martin, M.W., Matter, A., 2003. Extinction of *Cloudina* and *Namacalathus* at the Precambrian–Cambrian boundary in Oman. Geology 31, 431–434.

Bekker, A., Sial, A.N., Karhu, J.A., Ferreira, V.P., Noce, C.M., Kaufman, A.J., Romano, A.W., Pimentel, M.M., 2003. Chemostratigraphy of carbonates from the Minas Supergroup, Quadrilátero Ferrífero (Iron Quadrangle), Brazil: a stratigraphic record of Early Proterozoic atmospheric, biogeochemical and climatic change. Am. J. Sci. 303, 865–904.

Boggiani, P.C., 1998. Análise estratigráfica da Bacia Corumbá (Neoproterozoico)-Mato Grosso do Sul. Ph. D. Thesis, Universidade de São Paulo, Brazil, 181 pp.

Bossi, J., Campal, N., 1992. Magmatismo y tectónica transcurrente durante el Paleozoico Inferior en Uruguay. In: Gutierrez-Marco, J.G., Saavedra, J., Rabano, I. (Eds.), Paleozoico Inferior de Iberoamérica. Universidad de Extremadura, Mérida, pp. 343–356.

Bossi, J., Ferrando, L., Montaña, J., Campal, N., Morales, H., Gancio, F., Schipilov, A., Piñeyro, D., Sprechmann, P., 1998. Carta geológica del Uruguay. Escala 1:500.000. Geoeditores, Montevideo.

Bowring, S.A., Grotzinger, J.P., Isachsen, C.E., Knoll, A.H., Pelechaty, S.A., Kolosov, P., 1993. Calibrating rates of Early Cambrian evolution. Science 261, 1293–1298.

Brasier, M.D., 1996. U/Pb dates for the base of the terminal Proterozoic and Cambrian. Episodes 19 (3), 191.

Brasier, M.D., Lindsay, J.F., 2001. Did supercontinental amalgamation trigger the "Cambrian Explosion" ? In: Zhuravlev, A.Yu., Riding, R. (Eds.), The Ecology of Cambrian Radiation. Columbia Univ. Press, New York, pp. 69–89.

Brasier, M.D., Sukhov, S.S., 1998. The falling amplitude of carbon isotopic oscillation through the Lower and Middle Cambrian. Can. J. Earth Sci. 35, 353–373.

Brasier, M., Cowie, J., Taylor, M., 1994. Decision on the Precambrian–Cambrian boundary stratopype. Episodes 17, 3–8.

Brasier, M.D., Dorjnamjaa, D., Lindsay, J.F., 1996. The Neoproterozoic to early Cambrian in southwest Mongolia: an introduction. Geol. Mag. 133, 365–369.

Buggisch, W., Keller, M., Lehnert, O., 2003. Carbon isotope record of Late Cambrian to Early Ordovician carbonates of the Argentine Precordillera. Palaeogeogr. Palaeoclimatol. Palaeoecol. 195, 357–373.

Burns, S.J., McKenzie, J.A., Vasconcelos, C., 2000. Dolomite formation and biogeochemical cycles in the Phanerozoic. Sedimentology 47 (Suppl. 1), 49–61.

Cingolani, C., Spoturno, J., Bonhomme, M., 1990. Resultados mineralógicos preliminares sobre las unidades Piedras de Afilar, Lavalleja y Barriga Negra; R.O. del Uruguay. I Congreso Uruguayo Geología, Sociedad Uruguaya de Geología, Montevideo. Actas, vol. 1, pp. 11–17.

Corsetti, F.A., Kaufman, A.J., 1994. Chemostratigraphy of Neoproterozoic–Cambrian units, White-Inyo region, eastern California and western Nevada: implications for global correlation and faunal distribution. Palaios 9, 211–219.

Corsetti, F.A., Hagadorn, J.W., 2000. Precambrian–Cambrian transition: Death Valley, United States. Geology 28, 299–302.

Craig, H., 1957. Isotope standard for carbon and oxygen and correction factors for mass spectrometry analysis of carbon dioxide. Geochim. Cosmochim. Acta 12, 133–149.

Crimes, P.T., 1992. The record of trace fossils across the Proterozoic–Cambrian boundary. In: Lipps, J.H., Signor, P.W. (Eds.), Origin and early evolution of the Metazoa. Plenum Press, pp. 177–202.

Deer, W.A., Howie, R.A., Zussman, J., 1992. An Introduction to the Rock-forming MineralsSecond edition. Longman, Harlow. xvi + 696 pp., 237 figs.

Derry, L.A., Brasier, M.D., Corfield, R.M., Rozanov, A.Yu., Zhuravlev, A.Yu., 1994. Sr and C isotopes in Lower Cambrian carbonates from the Siberian craton: a paleoenvironmental record during the "Cambrian explosion". Earth Planet. Sci. Lett. 128, 671–681.

Dickson, T., 1990. Carbonate mineralogy and chemistry. In: Tucker, M.E., Wright, V.P. (Eds.), Carbonate sedimentology. Blackwell, Oxford, pp. 284–313.

Droser, M.L., Bottjer, D.J., 1988. Trends in depth and extent of bioturbation in Cambrian carbonate marine environments, western United States. Geology 16, 233–236.

Droser, M.L., Jensen, S., Gehling, J.G., Myrow, P.M., Narbonne, G.M., 2002. Lowermost Cambrian Ichnofabrics from the Chapel Island Formation, Newfoundland: implications for Cambrian Substrates. Palaios 17, 3–15.

Fedonkin, M.A., 2003. The origin of the Metazoa in the light of the Proterozoic fossil record. Paleontol. Res. 7, 9–41.

Gaucher, C., 2000. Sedimentology, palaeontology and stratigraphy of the Arroyo del Soldado Group (Vendian to Cambrian, Uruguay). Beringeria 26, 1–120.

Gaucher, C., Germs, G.J.B., 2002. Stepwise rifting of Rodinia as the prelude to the amalgamation of W-Gondwana? New insights from Uruguay and Brazil. 16th International Sedimentological Congress, Abstracts Volume. Johannesburg, pp. 111–112.

Gaucher, C., Schipilov, A., 1993. La secuencia arenosa-pelítica de Arroyo del Soldado. Rev. Bras. Geocienc. 23 (3), 312.

Gaucher, C., Sprechmann, P., 1999. Upper Vendian skeletal fauna of the Arroyo del Soldado Group, Uruguay. Beringeria 23, 55–91.

Gaucher, C., Sprechmann, P., Schipilov, A., 1996. Upper and Middle Proterozoic fossiliferous sedimentary sequences of the Nico Pérez Terrane of Uruguay: lithostratigraphic units, paleontology, depositional environments and correlations. Neues Jahrb. Geol. Palaäontol. Abh. 199, 339–367.

Gaucher, C., Sprechmann, P., Montaña, J., 1998. New advances on the geology and paleontology of the Vendian to Cambrian Arroyo del Soldado Group of the Nico Pérez Terrane of Uruguay. Neues Jahrb. Geol. Palaäontol., Monatsh. 1998 (2), 106–118.

Gaucher, C., Boggiani, P.C., Sprechmann, P., Sial, A.N., Fairchild, T.R., 2003. Integrated correlation of the Vendian to Cambrian Arroyo del Soldado and Corumbá Groups (Uruguay and Brazil): palaeogeographic, palaeoclimatic and palaeobiologic implications. Precambrian Res. 120, 241–278.

Gaucher, C., Sial, A.N., Blanco, G., Sprechmann, P., 2004a. Chemostratigraphy of the lower Arroyo del Soldado Group (Vendian, Uruguay) and palaeoclimatic implications. Gondwana Res. 7 (3), 715–730.

Gaucher, C., Sial, A.N., Pimentel, M.M., Ferreira, V.P., 2004b. Impact of a late Vendian, non-global glacial event on a carbonate platform, Polanco Formation, Uruguay. 1st Symposium on Neoproterozoic–Early Paleozoic Events in SW-Gondwana. Sao Paulo, pp. 21–23.

Germs, G.J.B., 1972. New shelly fossils from Nama Group, South West Africa. Am. J. Sci. 272, 752–761.

Germs, G.J.B., 1995. The Neoproterozoic of southwestern Africa, with emphasis on platform stratigraphy and paleontology. Precambrian Res. 73, 137–151.

Grant, S.W.F., 1990. Shell structure and distribution of *Cloudina*, a potential index fossil for the terminal Proterozoic. Am. J. Sci. 290-A, 261–294.

Grey, K., Walter, M.R., Calver, C.R., 2003. Neoproterozoic biotic diversification: Snowball Earth or aftermath of the Acraman impact? Geology 31, 459–462.

Hartmann, L.A., Santos, J.O., Bossi, J., Campal, N., Schipilov, A., Mac Naughton, N.J., 2002. Zircon and titanite U–Pb SHRIMP geochronology of Neoproterozoic felsic magmatism on the eastern

border of the Rio de la Plata Craton, Uruguay. J. South Am. Earth Sci. 15, 229–236.
Hoffman, P.F., Schrag, D.P., 2002. The snowball Earth hypothesis: testing the limits of global change. Terra Nova 14 (3), 129–155.
Hoffman, P.F., Kaufman, A.J., Halverson, G.P., Schrag, D.P., 1998. A Neoproterozoic snowball Earth. Science 281, 1342–1346.
Jacobsen, S.B., Kaufman, A.J., 1999. The Sr, C and O isotopic evolution of Neoproterozoic seawater. Chem. Geol. 161, 37–57.
Kah, L.C., Sherman, A.G., Narbonne, G.M., Knoll, A.H., Kaufman, A.J., 1999. $\delta^{13}C$ stratigraphy of the Proterozoic Bylot Supergroup, Baffin Island, Canada: implications for regional lithostratigraphic correlations. Can. J. Earth Sci. 36, 313–332.
Kaufman, A.J., Knoll, A.H., Semikhatov, M.A., Grotzinger, J.P., Jacobsen, S.B., Adams, W., 1996. Integrated chronostratigraphy of Proterozoic–Cambrian boundary beds in the western Anabar region, northern Siberia. Geol. Mag. 133, 509–533.
Kaufman, A.J., Knoll, A.H., Narbonne, G.M., 1997. Isotopes, ice ages and terminal Proterozoic earth history. Proc. Natl. Acad. Sci. U. S. A. 94, 6600–6605.
Kawashita, K., Gaucher, C., Sprechmann, P., Teixeira, W., Victória, R., 1999. Preliminary chemostratigraphic insights on carbonate rocks from Nico Pérez Terrane (Uruguay). Actas II South American Symposium on Isotope Geology. Córdoba, Argentina, pp. 399–402.
Knoll, A.H., 1994. Neoproterozoic evolution and environmental change. In: Bengtson, S. (Ed.), Early Life on Earth, Nobel Symposium, vol. 84. Columbia University Press, New York, pp. 439–449.
Knoll, A.H., 2000. Learning to tell Neoproterozoic time. Precambrian Res. 100 (2000), 3–20.
Landing, E., Bowring, S.A., Davidek, K.L., Westrop, S.R., Geyer, G., Heldmaier, W., 1998. Duration of the Early Cambrian: U–Pb ages of volcanic ashes from Avalon and Gondwana. Can. J. Earth Sci. 35, 329–338.
Logan, B.W., Rezak, R., Ginsburg, R.N., 1964. Classification and environmental significance of algal stromatolites. J. Geol. 72, 68–83.
Lund, K., Aleinikoff, J.N., Evans, K.V., Fanning, C.M., 2003. SHRIMP U–Pb geochronology of Neoproterozoic Windermere Supergroup, central Idaho: implications for rifting of western Laurentia and synchroneity of Sturtian glacial deposits. GSA Bull. 115, 349–372.
Melezhik, V.A., Gorokov, I.M., Kuznetsov, A.B., Fallick, A.E., 2001. Chemostratigraphy of Neoproterozoic carbonates: implications for "blind dating". Terra Nova 13, 1–11.
Montaña, J., Sprechmann, P., 1993. Calizas estromatolíticas y oolíticas y definición de la Formación Arroyo de la Pedrera (?Vendiano, Uruguay). Rev. Bras. Geocienc. 23, 306–312.
Montañez, I.P., Osleger, D.A., Banner, J.L., Mack, L.E., Musgrove, M., 2000. Evolution of the Sr and C isotope composition of Cambrian oceans. GSA Today 10 (5), 1–7.
Narbonne, G.M., Kaufman, A.J., Knoll, A.H., 1994. Integrated chemostratigraphy of the Windermere Supergroup, northwestern Canada: implications for Neoproterozoic correlations and the early evolution of animals. GSA Bull. 106, 1281–1292.
Peralta, S.H., 2000. Quebrada de Zonda Field Trip: The Cambrian carbonate sequence, litho and biostratigraphic features. Eastern Precordillera, San Juan, Argentina. In: Aceñolaza, G.F., Peralta, S.H. (Eds.), Cambrian from the Southern Edge. INSUGEO, Tucumán, pp. 21–28.
Pratt, B.R., Spincer, B.R., Wood, R.A., Zhuravlev, A.Yu., 2001. Ecology and evolution of Cambrian Reefs. In: Zhuravlev, A.Yu., Riding, R. (Eds.), The Ecology of Cambrian Radiation. Columbia Univ. Press, New York, pp. 254–274.
Riding, R., 1994. Evolution of algal and cyanobacterial calcification. In: Bengtson, S. (Ed.), Early life on earth — Nobel Symposium, vol. 84. Columbia University Press, New York, pp. 426–438.
Ryding, S.O., Rast, W., 1989. The Control of Eutrophication of Lakes and Reservoirs. UNESCO, Paris. 375 pp.
Shen, Y., Schidlowski, M., 2000. New C isotopic stratigraphy from southwest China: implications for the placement of the Precambrian–Cambrian boundary on the Yangtze Platform and global correlations. Geology 28, 623–626.
Sial, A.N., Peralta, S., Ferreira, V.P., Toselli, A.J., Aceñolaza, F.G., Parada, M.A., Gaucher, C., Alonso, R.N., Pimentel, M.M., 2003. C-, O- and Sr-isotope chemostratigraphy of Cambrian carbonate sequences, Precordillera, western Argentina. IV South American Symposium on Isotope Geology, Short Papers, vol. 1. CBPM, Salvador, pp. 390–393.
Sprechmann, P., Gaucher, C., Blanco, G., Montaña, J., 2004. Stromatolitic and trace fossils community of the Cerro Victoria Formation, Arroyo del Soldado Group (lowermost Cambrian, Uruguay). Gondwana Res. 7 (3), 753–766.
Steiner, M., 1994. Die neoproterozoischen Megaalgen Südchinas. Berl. geowiss. Abh., E Paläobiol. 15, 1–146.
Tucker, M.E., 1982. Precambrian dolomites: petrographic and isotopic evidence that they differ from Phanerozoic dolomites. Geology 10, 7–12.
Tucker, M.E., 1990a. Dolomites and dolomitization models. In: Tucker, M.E., Wright, V.P. (Eds.), Carbonate sedimentology. Blackwell, Oxford, pp. 365–400.
Tucker, M.E., 1990b. The geological record of carbonate rocks. In: Tucker, M.E., Wright, V.P. (Eds.), Carbonate sedimentology. Blackwell, Oxford, pp. 401–421.
Vasconcelos, C., McKenzie, J., 1997. Microbial mediation of modern dolomite precipitation and diagenesis under anoxic conditions (Lagoa Vermelha, Rio de Janeiro, Brazil). J. Sediment. Res. 67 (3), 378–390.
Veizer, J., 1994. The Archean–Proterozoic transition and its environmental implications. In: Bengtson, S. (Ed.), Early Life on Earth, Nobel Symposium No. 84. Columbia University Press, New York, pp. 208–219.
Vidal, G., Moczydlowska-Vidal, M., 1997. Biodiversity, speciation, and extinction trends of Proterozoic and Cambrian phytoplankton. Paleobiology 23 (2), 230–246.
Walter, M., 1994. Stromatolites: the main geological source of information on the evolution of the early benthos. In: Bengtson, S. (Ed.), Early life on earth — Nobel Symposium v. 84. Columbia University Press, New York, pp. 270–286.
Walter, M.R., Veevers, J.J., Calver, C.R., Gorjan, P., Hill, A.C., 2000. Dating the 840–544 Ma Neoproterozoic interval by isotopes of strontium, carbon and sulfur in seawater, and some interpretative models. Precambrian Res. 100, 371–433.
Weissert, H., Lini, A., Föllmi, K.B., Kuhn, O., 1998. Correlation of Early Cretaceous isotope stratigraphy and platform drowning events: a possible link? Palaeogeogr. Palaeoclimatol. Palaeoecol. 137, 189–203.
Zempolich, W.G., Baker, P.A., 1993. Experimental and natural mimetic dolomitization of aragonite ooids. J. Sediment. Petrol. 63, 596–606.
Zempolich, W.G., Wilkinson, B.H., Lohmann, K.C., 1988. Diagenesis of Late Proterozoic carbonates: the Beck Spring Dolomite of Eastern California. J. Sediment. Petrol. 58, 656–672.